Nano Research
DOI 10.1007/s12274-015-0894-8
Research Article

ISSN 1998-0124
CN 11-5974/O4

Flexible self-charging power unit by integrating micro-supercapacitor and triboelectric nanogenerator

Jianjun Luo[1,§], Feng Ru Fan[1,2,§], Tao Jiang[1], Zhiwei Wang[1], Wei Tang[1], Cuiping Zhang[1], Mengmeng Liu[1], Guozhong Cao[1,3], and Zhong Lin Wang[1,4] (✉)

Nano Res., **Just Accepted Manuscript** • DOI: 10.1007/s12274-015-0894-8
http://www.thenanoresearch.com on September 10 2015

Just Accepted

TSINGHUA UNIVERSITY PRESS Springer

TABLEOF CONTENTS (TOC)

Flexible Self-Charging Power Unit by Integrating Micro-supercapacitor and Triboelectric Nanogenerator

Jianjun Luo[1,†], Feng Ru Fan[1,2,†], Tao Jiang[1], ZhiweiWang[1], Wei Tang[1], CuipingZhang[1], MengmengLiu[1], GuozhongCao[1,3], Zhong Lin Wang[1,4*]

[1]Beijing Institute of Nanoenergy and Nanosystems, Chinese Academy of Sciences, Beijing 100083,China

[2]Collaborative Innovation Center of Chemistry for Energy Materials, College of Chemistry and Chemical Engineering, Xiamen University, Xiamen 361005, China

[3]Department of Materials Science and Engineering, University of Washington, Seattle,Washington 98195, USA

[4]School of Material Science and Engineering, Georgia Institute of Technology, Atlanta, Georgia 30332,USA

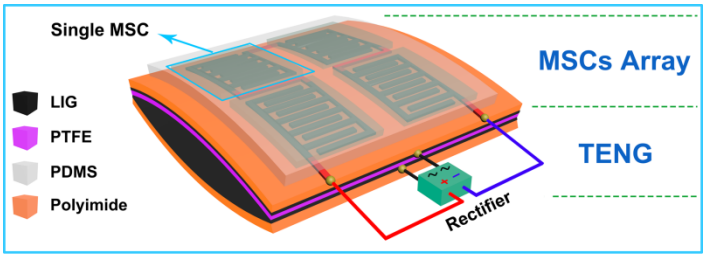

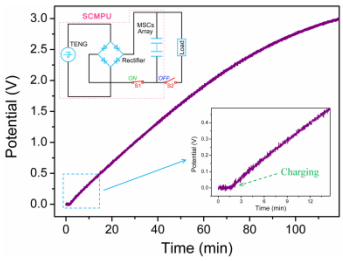

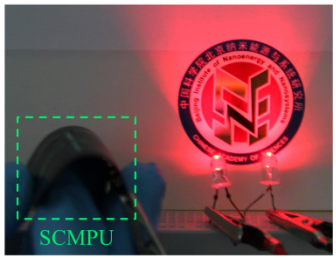

Using a simple and cost-effective laser engraving technique, we first attempted to fabricate a flexible self-charging micro-supercapacitor power unit (SCMPU) by integrating a TENG-based energy harvester and a MSCs array energy storage unit. The high degree of integration was realized through double-faced laser engraving on a polyimide (PI) substrate.

Zhong Lin Wang, http://www.nanoscience.gatech.edu/

Nano Research
DOI (automatically inserted by the publisher)
Review Article/Research Article **Please choose one**
ISSN 1998-0124
CN 11-5974/O4

Flexible self-charging power unit by integrating micro-supercapacitor and triboelectric nanogenerator

Jianjun Luo[1,†], Feng Ru Fan[1,2,†], Tao Jiang[1], ZhiweiWang[1], Wei Tang[1], CuipingZhang[1], MengmengLiu[1], GuozhongCao[1,3], Zhong Lin Wang[1,4](✉)

[1]*Beijing Institute of Nanoenergy and Nanosystems, Chinese Academy of Sciences, Beijing 100083,China*
[2]*Collaborative Innovation Center of Chemistry for Energy Materials, College of Chemistry and Chemical Engineering, Xiamen University, Xiamen 361005, China*
[3]*Department of Materials Science and Engineering, University of Washington, Seattle,Washington 98195, USA*
[4]*School of Material Science and Engineering, Georgia Institute of Technology, Atlanta, Georgia 30332,USA*
† These authors contributed equally to this work.

Received: day month year
Revised: day month year
Accepted: day month year (automatically inserted by the publisher)

KEYWORDS
energy harvesting,
energy storage,
Triboelectricnanogenerator,
micro-supercapacitor,
Self-charging,

ABSTRACT

The rapid development of portable and wearable electronic devices has increased demands for flexible and efficient energy harvesting and storage units. Conventionally, these two distinct processes are built as separated units and used as discrete components. Herein, we propose using a simple and cost-effective laser engraving technique to fabricate a flexible self-charging micro-supercapacitor power unit (SCMPU), by integrating a triboelectric nanogenerator (TENG) and a micro-supercapacitors (MSCs) array into a single device. The SCMPU is capable of beingdirectly charged up by ambient mechanical motion. In addition, it can be used to continuously power light-emitting diodes and a commercial hygrothermograph. This investigation will promote the development of sustainable self-powered systems and provide a new promising research branch for supercapacitors.

1 Introduction

Over the past decade, flexible, portable and wearable electronics have attracted increasing attention due to their rapid growing applications in various fields, such as electronic skin [1,2], soft robotics [3],medical

Address correspondence to zlwang@gatech.edu

diagnosis [4,5], and environmental monitoring [6,7]. Confronted with the serious problems of energy crisis and environmental pollution, the desire for fabricating green and renewable energy source for practical applications is becoming significantly important.Energy harvesting and storage, as the two most vital technologies for energy, are usually two different and separatedunits based on two consecutive processes.

In order to solve the problem of energy harvesting, the piezoelectric nanogenerator (PNG) [8,9] has been developed in 2006to efficiently convert low-frequency mechanical energy into electricity. Additionally, a new concept of a self-charging power cell [10-13] was introduced through which mechanical energy can be directly converted into electrochemical energy and stored. However, the main limitation of these devices is that the PNG does not possess a sufficient amount of power to charge the connected large-capacity storage unit. Most recently, a novel energy-harvesting device named triboelectric nanogenerator (TENG) [14-16] has been invented and widely utilized to efficiently scavenge mechanical energy. The working mechanism of the TENG is based on the coupling effect of contact electrification and electrostatic induction [17,18].In addition, a self-charging power unit [19] integrated with an TENG and a Li-ion battery has been reported in literature.

With the rapid development of miniaturized electronic devices, all-solid-statemicro-supercapacitors (MSCs) have proven to have great potential to complementor replace batteries and electrolytic capacitors in a variety of applications [20-22], owing to its remarkable advantages of high-power density, high-rate capability, long cycle life, and environmentally benign.From the materials point of view, graphene offers tremendous potential for energy storage because of its high surface area and superior electrical conductivity [23]. Recently, a simple, inexpensive method to produce laser-induced graphene (LIG) has been developed and implemented in the fabrication of high-performance supercapacitors [24,25]. Unfortunately, the inevitable problem of conventional supercapacitors is the limited lifetime. In this context, finding a simple and cost-efficient method to fabricate a flexible self-charging micro-supercapacitor power unit may sufficiently meet the demands of small-sized, portable electronics.

In consideration of the problems described above, we first attempted to fabricate a flexible self-charging micro-supercapacitor power unit (SCMPU) using a laser engraving technique by integrating a TENG-based energy harvester and a MSCs array energy storage unit. The high degree of integration was realized through double-faced laser engraving on a polyimide (PI) substrate. Thus, the different sides of the LIG electrodes can be respectively used for fabricating the TENG and MSCs array. When the ambient stress is applied onto the SCMPU, the mechanical energy will be directly converted into electrical energy and storedin the MSCs array,which can be charged to 3 V in 117min. Remarkably, the device demonstrated herein behaves with exceptional mechanical durability and electrochemical stability, even under different bending and pressing conditions. When fully charged, the SCMPU can continuously power two light-emitting diodes (LEDs) or a commercial hygrothermograph. The designed SCMPU proves to have great potential for powering wearable electronics, medical devices, and environmental/infrastructure sensors.

2Result and discussion

The device structure of the SCMPU is schematically depicted in Fig. 1(a). The entire device is composed of two primary components: a flexible MSCs array and an arched structure TENG. These two parts were highly integrated through the double-faced laser engraving on the top PI substrate via a commercial CO_2 laser cutter system, while the different sides of the LIG electrodes were used to fabricate the TENG and MSCs array, respectively. The schematic diagram of the laser engraving process is shown in Fig. S1. Fig. 1(b) is the cross-sectional scanning electron microscope (SEM) images of the double-sided laser-engraved PI

substrate. It should be noted that the LIG layers on both sides are ~40μm and are separated by an unexposed middle PI substrate that serves to electrically isolate the two sides of LIG from each other. The higher magnification SEM image (inset of Fig. 1(b)) displays a porous, multilayer structure of the cross-sectional LIG. Also, SEM images in Fig. 1(c) show the surface topography of the LIG that reveala regular, porous microstructure written by the laser system, which is beneficial to improve the performance of both the MSCs array and the TENG. Moreover, high-resolution transmission electron microscopy (HRTEM) image in Fig. 1(d) reveals few-layer features and highly ripple-like wrinkled structures of the thin LIG flakes. The above characterizations of LIG showed similar morphology and graphene properties to the previous report [24].

A photograph of a typical SCMPU device is shown in the inset (top) of Fig. 1(a), clearly revealing its flexibility and arch-shaped structure. The dimension of the SCMPU is 3 cm × 3 cm, which of course can be further reduced in size due to the high resolution of the laser system. To increase the triboelectric charge density through a large surface area and to enhance the mechanical robustness of the TENG, the surface of the polytetrafluoroethylene (PTFE) thin film was modified with a layer of PTFE nanoparticles [26], as illustrated in the inset (bottom) of Fig. 1(a). With this highlyintegrated SCMPUstructure, the MSCs array can be fully charged through harvestingambient mechanical energy by solely rectifying theTENG-generated alternatingcurrent (AC) pulses todirect current(DC) with a low loss full-wave bridge rectifier. The working principle of the SCMPU is charted in Fig. S2 and the detailed fabrication process is described in the following Experimental section.

To ensure the feasibility of the proposed device'sstructure, an energy harvesting portion with high output performance is essential. Therefore, it is imperative to first characterize the outputs of the LIG triboelectric nanogenerator (LIG-TENG). The electrical output measurement of the LIG-TENG was carried out by a linear mechanical motor under a frequency of 0.6 Hz. In the process of contact-separation, the open-circuit voltage (V_{OC}) of ~168 V was generated between the two electrodes of the LIG-TENG (Fig. 2(a)). The transferred charge density ($\Delta\sigma$) of ~68 μC/m^{2}driven by this potential difference was also measured, as shown in Fig. 2(b). Consequently,the transfer of the charges produced an AC output with a peak short-circuit current density (J_{SC}) of 21.3mA/m^2 corresponding to the contact-separation process (Fig. 2(c)).

To further investigate the stability of the LIG-TENG,a periodical pressure with a frequency of 1 Hz was applied. The voltage was recorded after each 10,000 loading/unloadingcycles and 300 cycles of data were presented in each recording,as shown in Fig. 2(d). The voltage amplitudes exhibit negligiblechange after a total of 40,000 cycles, revealing high repeatability,stability, and durability of the LIG-TENG unit.

Fig. 2(e) illustrates the dependence of both voltage and current density outputs on a series of different resistances(from 10^3 Ω to 2 GΩ). It is evident that the current density drastically decreases as the external resistance increases, while the voltage across the load behaves in a reverse manner. Consequently, the effective electrical power density of the LIG-TENG is closely related to the external load and reaches a maximum value of 0.8 W/m^2 at a load resistance of 20 MΩ (Fig. 2(f)). Thus, the output performance of this LIG-TENG is comparable to the conventional metal-based TENG [27,28] and much higher than the reported graphene-based TENG [29]. Most importantly, it has obvious advantages of being simple, cost-effective, and scale-controllable. In addition, this technique may have a promising prospect in the application of TENGs in other modes [30], such as lateral-sliding mode and freestanding triboelectric-layer mode, due to the easily patterned LIG electrodes.

In order to further validate the feasibility of the device's structural design, we need to characterize the performance of the LIG micro-supercapacitor (LIG-MSC). The device's architecture of the fabricated all-solid-state LIG-MSC is shown in Fig. 3(a) and the detailed fabrication process is described in the Experimental section. Fig. 3(b) displays a photograph of the as-prepared LIG electrodes (single and four connected in series). A single LIG-MSC was

constructed with 10 interdigitated microelectrodes, which include 5 positive and 5 negative electrodes. The cyclic voltammetry (CV) curves at different scan rates (5, 10, 20, and 50 mV/s), which exhibit capacitive behavior with a quasi-rectangle shape, are shown in Fig. 3(c), suggestive of electrochemical double layer (EDL) stability. Additionally, Fig. 3(d) shows the galvanostatic charge-discharge (CC) curves at varying current densities ranging from 0.02 to 0.20 mA/cm^2. Note that the CC curves are nearly an ideal triangular shape that is indicative ofsuperior capacitive behavior. Inspection of the beginning of each discharge curve shows a negligible voltage drop that implies a very low internal resistance of the device.

The areal capacitances (C_A) of the LIG-MSC is calculated from the CC curves by the following equations:

$$C = I\Delta t/\Delta V \quad (1)$$

$$C_A = C/S = I\Delta t/S\Delta V \quad (2)$$

where C is the total capacitance, I is the discharge current, Δt is the discharge time, ΔV is the potential window on discharging after IR drop, and S represents the total area of the active positive and negative electrodes. It can be seen that the C_A is ~10.29 mF/cm^2 at a current density of 0.01 mA/cm^2 (Fig. 3(e)), comparable or higher than those reported in the literature for carbon-based MSCs [21,22,24,31,32]. Furthermore, the single LIG-MSC shows excellent cycling stability, retaining 97% of the initial capacitance after 10,000 charge/discharge cycles (Fig. 3(f)). Atypical galvanostatic CC curve under continuous operation forthe last10 cycles is shown in the inset of Fig. 3(f). As can be seen from the above results, the LIG-MSC displayedsuperior performance that deems it suitable for the integration of the self-charging system.

Considering the SCMPU would maintain at bended and pressed state cyclically while working, we ought to further demonstrate the durability of the LIG-MSC. Fig. 4(a) illustrates photographs showing the LIG-MSC was placed under mechanical stress of bending and pressing. The CV performance of the LIG-MSC when tested under different bending and pressing conditions is shown in Fig. 4(b). No apparent changes of the CV curves were observed, indicative of the bending and pressing having a negligible effect on the capacitive behavior of the LIG-MSC. The performance durability can be primarily attributed to the highly mechanical flexibility of the all-solid-state LIG-MSC system and the adequate elasticity of the PDMS as a protective layer. Additionally, the C_A of the LIG-MSC was tested while keeping the device under the bended or pressed state. Remarkably, the capacitance was well-maintained at 98% of its initial capacitance after 6,000 cycles (Fig. 4(c)). These findings further demonstrate that the LIG-MSC is a promising candidate for energy storage devices in flexible, portable, and wearable electronics.

Practical applications often require energy storage units packaged either in series, in parallel, or in combinations of the two in order to meet energy power requirements. Thus, MSCs arrays connected with four single MSCs in series and/or parallel configurations were designed by the computer controlled laser system. As shown in Fig. 4(d-f), the operating potentials and currents can be well controlled by different configurations. Identical to the single MSC, the MSCs arrays reveal essentially perfect triangular CC curves with a miniscule voltage drop,indicativeof excellent capacitive properties and negligible internal resistance. Moreover, the MSCs arraysexhibit excellent cycling stability (Fig. S3). Considering the resolution of the controllable laser system, the size of a single MSC can be further reduced and the MSCs array can be easily adjusted to various combinations depending on the specific application (Movie S1).

In order to preferably match the MSCs array, the output voltage of the LIG-TENG needs to be reduced. Presently, there are two methods to reduce the output voltage of the TENG. The first method is to use a transformer [33]. However, the use of a transformer not only causes substantial energy loss but also adds unnecessary weight and volume to the system. Furthermore, it is difficult to match the low-frequency and high-output load resistance properties of the TENG. Another method is to reduce the voltage by reducing the gap distance (d) of the TENG, which was proven successful in our previous works [34,35]. Obviously, the second option is much

more efficient for the self-charging system. To theoretically investigate the V_{OC}-d relationship of the LIG-TENG, a numerical calculation with finite element method (FEM) was performed on the system. For simplicity purposes, the LIG-TENG is treated as a parallel-plate capacitor in theestablished model where the PTFE plate with LIG electrode was placed parallel with thecounter LIG plate withvariable gap distances ranging from 0 to 24μm. Thetriboelectric charge density on the inner surface ofPTFE plate was assigned as 68μC/m^2, equalingto the measured transferred charge density from Fig. 2(b). The calculated potential distribution aroundthe parallel-plate structure is displayedwith color scalingin Fig. 5(a-d). It can be found that the potentialdifference between the top and bottom electrodesshows a clear decreasing trend with decreasinggap distance. By utilization of the numerical calculations, the experimental gap distance of the LIG-TENG was reduced and the results are shown in Fig. 5(e-f). When reducing the gap distance of the TENG component, the $V_{OC}$was reduced to ~30 V, which can effectively match the MSCs array while the J_{SC} was reduced to ~1.5 mA/m^2. This AC output can be rectified to unidirectional pulse output by a low-loss full wave bridge rectifier (Fig. 5(g)) that generates electricity to be stored in the MSCs array component. While working in the energy harvesting mode (top inset of Fig. 5(h), S1 on; S2 off), the SCMPU can convert the mechanical energy to electrical energy and store it in the MSCs array component. The charging curve of the MSCs array component is shown in Fig. 5(h). It can be seen that the storage charges steadily increase with an increase in the charging time and the potential reaches 3 V in 117 min.

When a sufficient amount of charge has been stored duringthe energy storage mode, the SCMPU will progress to the energy supply mode (S1 off; S2 on). The circuit diagram of the energy supply mode is displayed in Fig. 6(a). Fig. 6(b) exhibits that the fully charged SCMPU was directly used to simultaneously power two light-emitting diodes (LEDs) with a minimum operating potential of 1.5 V. The painted area demonstrates the flexibility of the device. Even when bentto 90°, the device can still work in its normal behavior. Besides, the SCMPU can be inserted into the insole of a shoe (Fig. 6(c)),indicating its potential applications for wearable electronics. To further demonstrate the application of the SCMPU,it was successfully utilized to continuously power a commercial hygrothermograph(Fig. 6(d-f)). The apparent difference of the temperature and degree of humidity between indoor and outdoor was measured.

3Conclusion

In summary, using a simple and cost-effective laser engraving technique, we have developed a flexibleself-charging micro-supercapacitor power unit(SCMPU) that highly integrates a triboelectric-based energy harvesting unit and an electrochemical storage unit into a single device. The SCMPU exhibits remarkable advantages such as self-charging, high durability, and it is environmentally friendly. The LIG-TENGhas a peak power density of 0.8 W/m^2 at a loading resistance of 20 MΩ. Additionally, the MSC has a high capacitance of ~10.29 mF/cm^2 at a current density of 0.01 mA/cm^2. As triggered by ambient mechanical vibrations, the TENG component can efficiently generate electricity with high output and the rectified electrical energy is directly stored in the MSCs array component,which can be charged to 3 V in 117min. When fully charged, the SCMPU can continuously power two LEDs and a commercial hygrothermograph.This work demonstrates a milestone in the development of mobile energy and will have a profound influence on self-powered systems for flexible and wearable electronic devices.

Experimental section

Preparation of the polymer electrolyte. In a typical process, 5 mL ofH_2SO_4 (98 wt %, Sigma Aldrich) and 5 g ofPoly(vinyl alcohol)powder(Mw=50000, Sigma Aldrich) were added to 50 mL ofDI water. Subsequently, thewhole mixture was heated to 80 °C under continuous stirring until thesolution became clear.

Fabrication of the MSC.LIG electrodes were directly

written onto surface of the Kapton polyimide (PI, DuPont, 125μm) substrates with a CO_2 laser cutter system (Universal PLS-6.75 laser system). Laser power was controlled at 5.0 W in all the experiments. The PI substrates were first ultrasonically cleaned in acetone, ethanol, and DI water for 30 min each other. In the MSC, LIG serves as both the active electrode and current collectors. For better electrical connection, silver paint was applied on the edges of the positive and negative electrodes. The electrodes were extended with copper tapes. The interdigital area is defined with polyethylene terephthalate (PET) tape to protect the contact pad from the electrodes. Next, the electrolyte was drop-cast on the active interdigitated electrode area, and left under ambient conditions for 12 h to ensure that the electrolyte completely wets the electrodes and to remove the excess water by evaporation. Finally, fluidPDMS (Sylgard 184, Tow Corning) was spin-coated (at 500rpm) onto the LIG-MSCs and cured at room temperature for 24 h.

Fabrication of the SCMPU.PI substrates are divided into two groups (named as PI 1 and PI 2) for different fabrication processes. For PI 1, LIG electrodes were produced on its both sides. Firstly, upper surface is for the MSCs array. MSCs array is fabricated with the same process used in the above in MSC fabrication process, except for the four written LIG patterns connected in series. Then, LIG was produced on the other side of PI 1 with an area of 3 cm × 3 cm as the top electrode. A layer of FTFE film was pasted on the LIG. Finally, water-based PTFE nanoparticle suspension was evenly sprayed onto the PTFE film, and dried by air blow. For PI 2, LIG was produced on its single side with an area of 3 cm × 3 cm as the bottom electrode. In the end, PI 1 was placed onto PI 2, with PTFE surface and LIG electrode face to face. And the whole device was sealed at the two ends, forming an arched structure.

Characterization and Measurement.SEM images were characterized using a HITACHI SU8020 and a FEI Quanta 450 FEG FE-SEM. High-resolution TEM image was characterized using a FEI Tecnai G2 F20 S-TWIN TMP FE-TEM. The V_{OC}, J_{SC} and $\Delta\sigma$ were measured by theKeithley 6514 electrometer. CV measurements wereperformed using an Autolab PGSTAT302N electrochemical workstation. Galvanostatic CC measurements were performed using the LANHE CT2001A battery testing system.

Acknowledgements

This research was supported by National Natural Science Foundation of China (Grant Nos.51432005 and 21403181), the "thousands talents" program for pioneer researcher and his innovation team, China, and Beijing City Committee of science and technology project (Grant Nos. Z131100006013004 and Z131100006013005). The authors would like to thank Chao Yuan, Weiming Du and Yaguang Liufor helpful discussions and assistance in experiments.

Electronic Supplementary Material:Supplementary materialis available in the online version of this article at http://dx.doi.org/10.1007/s12274-***-****-*

References

[1] Mannsfeld, S. C. B.;Tee, B. C. K.;Stoltenberg, R. M.;Chen, C. V. H. H.;Barman, S.;Muir, B. V. O.;Sokolov, A. N.;Reese, C.; Bao, Z. Highly sensitive flexible pressure sensors with microstructured rubber dielectric layers. Nat. Mater. 2010, 9, 859-864.

[2] Kang, D.;Pikhitsa, P. V.;Choi, Y. W.;Lee, C.;Shin, S. S.;Piao, L.;Park, B.;Suh, K.-Y.;Kim, T.i.; Choi, M. Ultrasensitive mechanical crack-based sensor inspired by the spider sensory system. Nature 2014, 516, 222-226.

[3] Ilievski, F.;Mazzeo, A. D.;Shepherd, R. E.;Chen, X.; Whitesides, G. M. Soft Robotics for Chemists. Angew. Chem. Int. Ed. 2011, 50, 1890-1895.

[4] Jeong, J.W.;Yeo, W.H.;Akhtar, A.;Norton, J. J. S.;Kwack, Y.J.;Li, S.;Jung, S.Y.;Su, Y.;Lee, W.;Xia, J.;Cheng, H.;Huang, Y.;Choi, W.S.;Bretl, T.; Rogers, J. A. Materials and Optimized Designs for Human-Machine Interfaces Via Epidermal Electronics. Adv. Mater. 2013, 25, 6839-6846.

[5] Chen, L. Y.;Tee, B. C. K.;Chortos, A. L.;Schwartz, G.;Tse, V.;Lipomi, D. J.;Wong, H. S. P.;McConnell, M. V.; Bao, Z. Continuous wireless pressure monitoring and mapping with ultra-small passive sensors for health monitoring and critical care. Nat. Commun. 2014, 5, 5028.

[6] Lee, M.;Bae, J.;Lee, J.;Lee, C.S.;Hong, S.; Wang, Z. L. Self-powered environmental sensor system driven by nanogenerators. Energy Environ. Sci. 2011, 4, 3359-3363.

[7] Pang, C.;Lee, G.Y.;Kim, T.i.;Kim, S. M.;Kim, H. N.;Ahn, S.H.; Suh, K.Y. A flexible and highly sensitive strain-gauge sensor using reversible interlocking of nanofibres. Nat. Mater. 2012, 11, 795-801.

[8] Wang, Z. L.; Song, J. H. Piezoelectric nanogenerators based on zinc oxide nanowire arrays. Science 2006, 312,

242-246.

[9] Wang, X. D.;Song, J. H.;Liu, J.; Wang, Z. L. Direct-current nanogenerator driven by ultrasonic waves. Science 2007, 316, 102-105.

[10] Xue, X. Y. ;Wang, S. H.;Guo, W. X.;Zhang, Y.; Wang, Z. L. Hybridizing Energy Conversion and Storage in a Mechanical-to-Electrochemical Process for Self-Charging Power Cell. Nano Lett. 2012, 12, 5048-5054.

[11] Xue, X. Y.;Deng, P.;He, B.;Nie, Y. X.;Xing, L. L.;Zhang, Y.; Wang, Z. L. Flexible Self-Charging Power Cell for One-Step Energy Conversion and Storage. Adv. Energy Mater.2014, 4, 1301329.

[12] Xing, L. L.;Nie, Y. X.;Xue, X. Y.; Zhang, Y. PVDF mesoporous nanostructures as the piezo-separator for a self-charging power cell. Nano Energy 2014, 10, 44-52.

[13] Ramadoss, A.;Saravanakumar, B.;Lee, S. W.;Kim, Y.S.;Kim, S. J.; Wang, Z. L. Piezoelectric-driven self-charging supercapacitor power cell. ACS nano 2015, 9, 4337-4345.

[14] Fan, F. R.;Tian, Z. Q.; Wang, Z. L. Flexible triboelectric generator. Nano Energy 2012, 1, 328-334.

[15] Wang, Z. L. Triboelectric Nanogenerators as New Energy Technology for Self-Powered Systems and as Active Mechanical and Chemical Sensors. AcsNano 2013, 7, 9533-9557.

[16] Fan, F. R.;Luo, J. J.;Tang, W.;Li, C. Y.;Zhang, C. P.;Tian, Z. Q.; Wang, Z. L. Highly transparent and flexible triboelectric nanogenerators: performance improvements and fundamental mechanisms. J. Mater. Chem. A 2014, 2, 13219-13225.

[17] Grzybowski, B. A.;Winkleman, A.;Wiles, J. A.;Brumer, Y.; Whitesides, G. M. Electrostatic self-assembly of macroscopic crystals using contact electrification. Nat. Mater. 2003, 2, 241-245.

[18] Zhu, G.;Pan, C. F.;Guo, W. X.;Chen, C.Y.;Zhou, Y. S.;Yu, R. M.; Wang, Z. L. Triboelectric-Generator-Driven Pulse Electrodeposition for Micropatterning. Nano Lett. 2012, 12, 4960-4965.

[19] Wang, S. H.;Lin, Z.H.;Niu, S. M.;Lin, L.;Xie, Y. N.;Pradel, K. C.; Wang, Z. L. Motion Charged Battery as Sustainable Flexible-Power-Unit. AcsNano 2013, 7, 11263-11271.

[20] Chmiola, J.;Largeot, C.;Taberna, P.L.;Simon, P.; Gogotsi, Y. Monolithic Carbide-Derived Carbon Films for Micro-Supercapacitors. Science 2010, 328, 480-483.

[21] Gao, W.;Singh, N.;Song, L.;Liu, Z.;Reddy, A. L. M.;Ci, L. J.;Vajtai, R.;Zhang, Q.;Wei, B. Q.; Ajayan, P. M. Direct laser writing of micro-supercapacitors on hydrated graphite oxide films. Nat. Nanotechnol. 2011, 6, 496-500.

[22] El-Kady, M. F.; Kaner, R. B. Scalable fabrication of high-power graphene micro-supercapacitors for flexible and on-chip energy storage. Nat. Commun. 2013, 4, 1475.

[23] Zhu, Y. W.;Murali, S.;Stoller, M. D.;Ganesh, K. J.;Cai, W. W.;Ferreira, P. J.;Pirkle, A.;Wallace, R. M.;Cychosz, K. A.;Thommes, M.;Su, D.;Stach, E. A.; Ruoff, R. S. Carbon-Based Supercapacitors Produced by Activation of Graphene. Science 2011, 332, 1537-1541.

[24] Lin, J.;Peng, Z. W.;Liu, Y. Y.;Ruiz-Zepeda, F.;Ye, R. Q.;Samuel, E. L. G.;Yacaman, M. J.;Yakobson, B. I.; Tour, J. M. Laser-induced porous graphene films from commercial polymers. Nat. Commun. 2014, 5, 5714.

[25] Peng, Z. W.;Lin, J.;Ye, R. Q.;Samuel, E. L. G.; Tour, J. M. Flexible and Stackable Laser-Induced Graphene Supercapacitorse. Acs Appl. Mater. Interfaces 2015, 7, 3414-3419.

[26] Zhu, G.;Zhou, Y. S.;Bai, P.;Meng, X. S.;Jing, Q. S.;Chen, J.; Wang, Z. L. A Shape-Adaptive Thin-Film-Based Approach for 50% High-Efficiency Energy Generation Through Micro-Grating Sliding Electrification. Adv. Mater. 2014, 26, 3788-3796.

[27] Wang, S. H.;Lin, L.; Wang, Z. L. Nanoscale Triboelectric-Effect-Enabled Energy Conversion for Sustainably Powering Portable Electronics. Nano Lett. 2012, 12, 6339-6346.

[28] Zhang, C.;Zhou, T.;Tang, W.;Han, C. B.;Zhang, L. M.; Wang, Z. L. Rotating-Disk-Based Direct-Current Triboelectric Nanogenerator. Adv. Energy Mater.2014, 4, 1301798.

[29] Kim, S.;Gupta, M. K.;Lee, K. Y.;Sohn, A.;Kim, T. Y.;Shin, K.S.;Kim, D.;Kim, S. K.;Lee, K. H.;Shin, H.J.;Kim, D.W.; Kim, S.W. Transparent Flexible Graphene Triboelectric Nanogenerators. Adv. Mater. 2014, 26, 3918-3925.

[30] Wang, S. H.;Lin, L.; Wang, Z. L. Triboelectric nanogenerators as self-powered active sensors. Nano Energy 2015, 11, 436-462.

[31] Pech, D.;Brunet, M.;Durou, H.;Huang, P.;Mochalin, V.;Gogotsi, Y.;Taberna, P.L.; Simon, P. Ultrahigh-power micrometre-sized supercapacitors based on onion-like carbon. Nat. Nanotechnol. 2010, 5, 651-654.

[32] Wu, Z.S.;Parvez, K.;Feng, X. L.; Muellen, K. Graphene-based in-plane micro-supercapacitors with high power and energy densities. Nat. Commun. 2013, 4, 2487.

[33] Zhu, G.;Chen, J.;Zhang, T. J.;Jing, Q. S.; Wang, Z. L. Radial-arrayed rotary electrification for high performance triboelectric generator. Nat. Commun. 2014, 5, 3426.

[34] Lin, L.;Xie, Y. N.;Wang, S. H.;Wu, W. Z.;Niu, S. M.;Wen, X. N.; Wang, Z. L. Triboelectric Active Sensor Array for Self-Powered Static and Dynamic Pressure Detection and Tactile Imaging. AcsNano 2013, 7, 8266-8274.

[35] Luo, J. J.;Fan, F. R.;Zhou, T.;Tang, W.;Xue, F.; Wang, Z. L. Ultrasensitive self-powered pressure sensing system. Extreme Mech. Lett. 2015, 2, 28-36.

Figures and figure captions

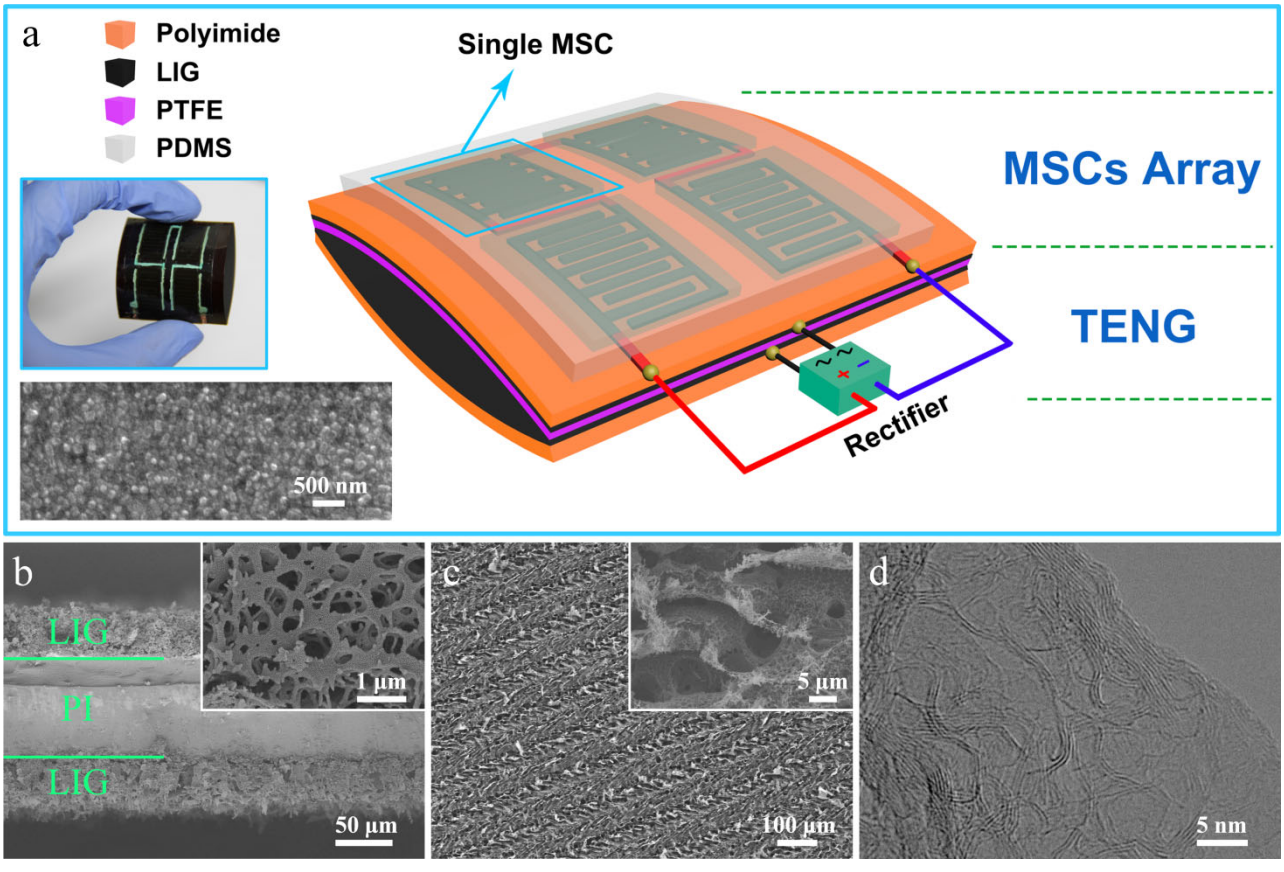

Figure 1 (a) Schematic diagram depicting the detailed structureof the SCMPU, top inset is the photograph of a SCMPU, bottom inset is an SEM image of PTFE nanoparticles applied onto the surface of PTFE film. (b) Cross-sectional SEM image of a double-sided laser-engraved PI substrate with both sides LIG, inset is the enlarged SEM image showing the porous, multilayer morphology of LIG. (c) SEM image of the LIG thin film, inset is the enlarged SEM image. (d) HRTEM image taken at the edge of a LIG flake.

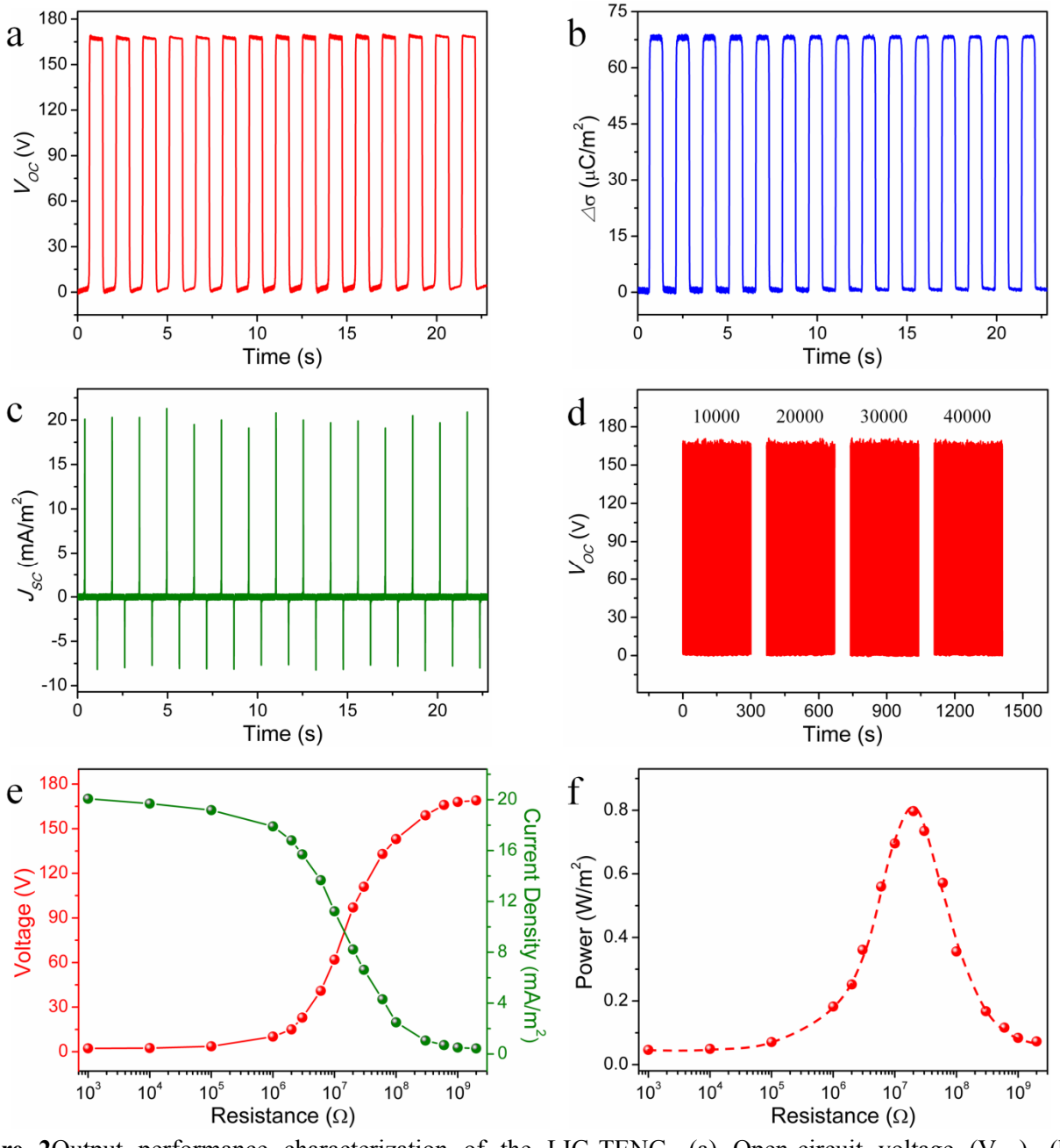

Figure 2 Output performance characterization of the LIG-TENG. (a) Open-circuit voltage (V_{OC}), (b) transferred charge density ($\Delta\sigma$), and (c) short-circuit current density (J_{SC}) generated by the LIG-TENG under a periodical deformation frequency of 0.6 Hz. (d) The mechanical durability characterizationof the LIG-TENG. At a frequency of 1 Hz for 40,000 cycles, no degradation of the output voltage isexperimentally observed. (e) The dependence of the output voltage and current density, and (f) instantaneous power density of the LIG-TENG on theresistance ofexternal load.

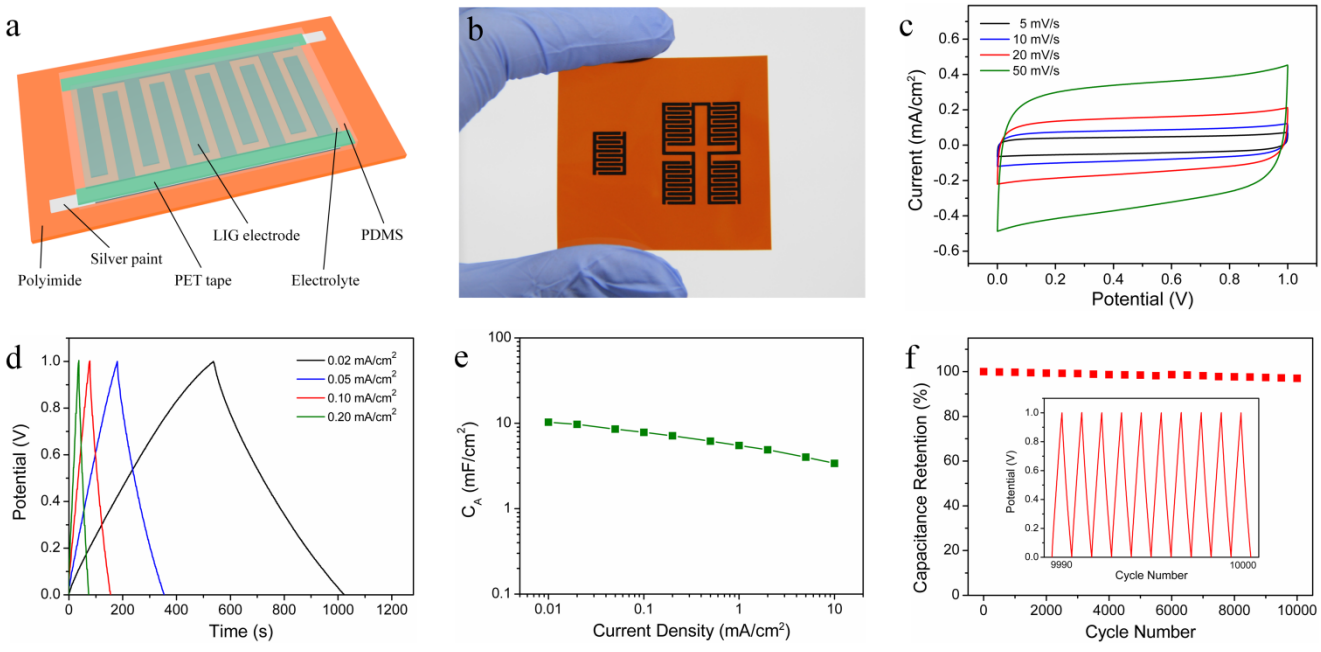

Figure 3(a) Schematic diagram and electrochemical performance of a single all-solid-state LIG-MSCdevice architecture. (b) Photograph of the LIG interdigitated electrodes (single and four connected in series). (c) CV curves of LIG-MSCs at scan rates of 5, 10, 20, and 50 mV/s. (d) Galvanostatic CC curves of LIG-MSCs at current densities of 0.02, 0.05, 0.10, and 0.20 mA/cm^2. (e) Specific areal capacitances (C_A) calculated from CC curves as a function of the current density. (f) Cyclability testing of LIG-MSC with a CC current density of 0.05 mA/cm^2, demonstrating only 3% loss of its initial capacitance over 10,000 cycles. Inset shows the galvanostatic CC curves for the last 10 cycles.

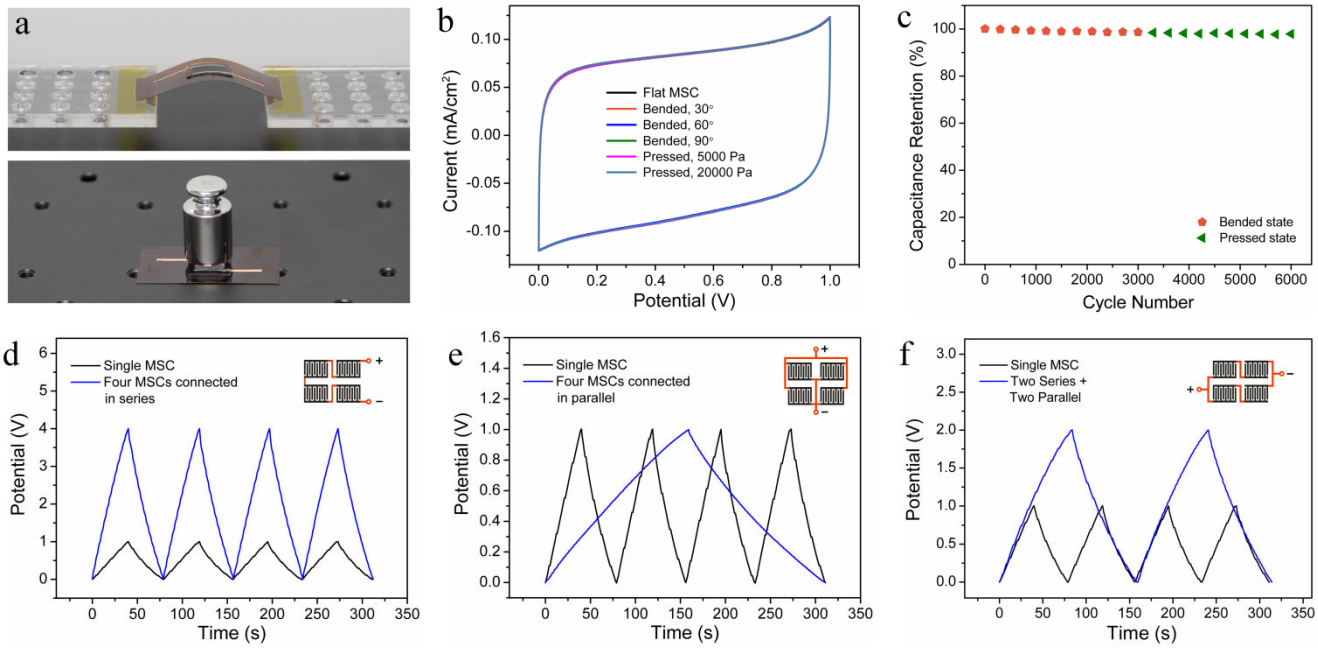

Figure 4(a) Photographs of LIG-MSC bentto 30° and pressed with 5,000 Pa. (b) Bending/pressing the LIG-MSC has almost no effect on its performance as demonstrated from the CV curves collected under different bending and pressing conditions at 10 mVs^{-1}. (c) Performance durability of the MSC when tested under bending and pressing conditions (60° and 20,000 Pa) with current density of 0.05 mA/cm^2. The device retains ~98% of its initial capacitance after 3,000 cycles under a bended state, followed by another 3,000 cycles under the pressed state. (d-f) Galvanostatic CC curves of different MSCs arrays (four single MSCs connected in series, parallel, combination of series and parallel, respectively) at current density of 0.10 mA/cm^2. A single MSC is shown for comparison purposes.

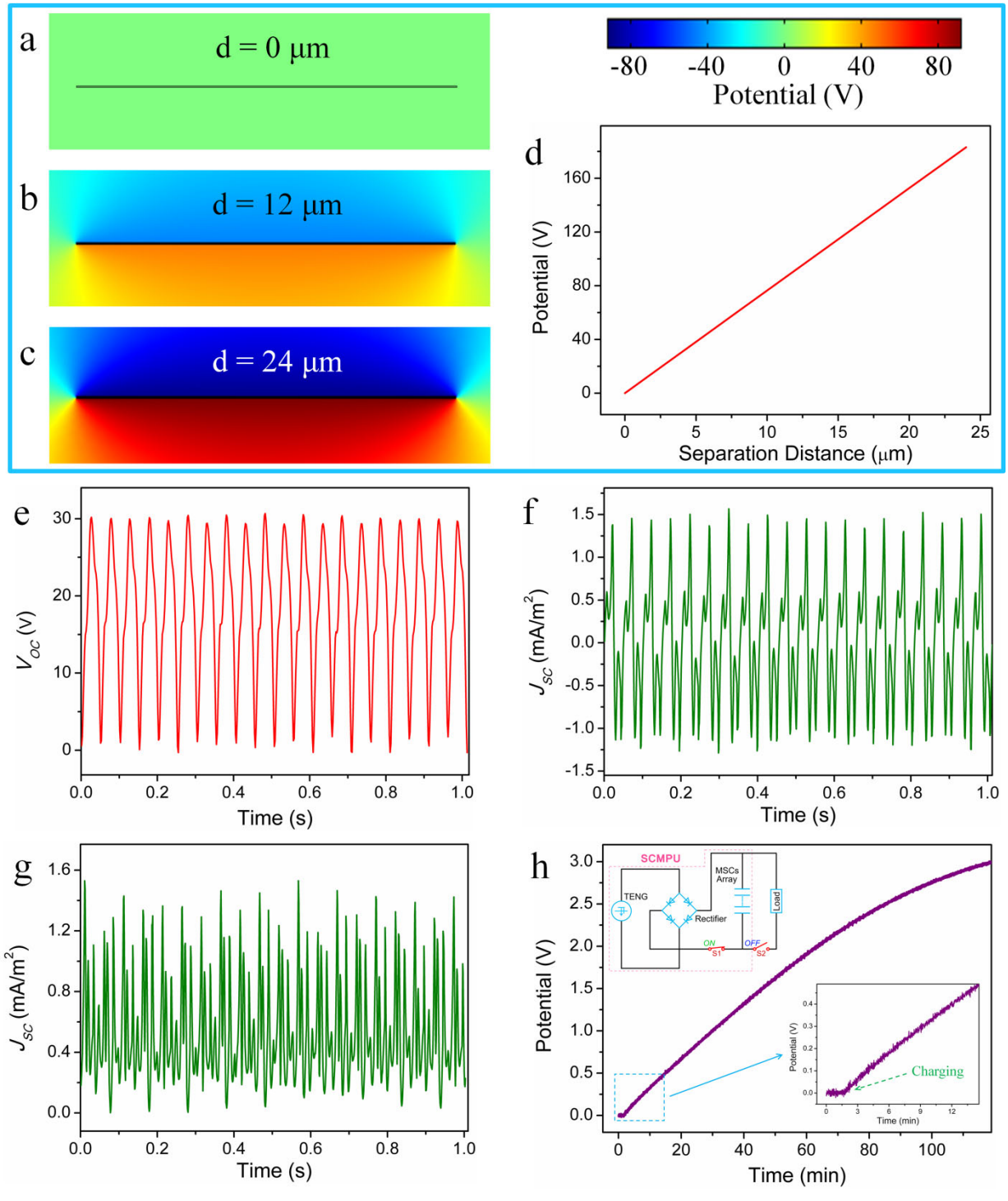

Figure 5(a-d) Numerical calculations of the correlation between the potential difference and the gap distance of theLIG-TENG. (e) V_{OC}, (f) J_{SC}, and (g) rectified J_{SC} generated by the TENG component when reducing the gap distance. (h) Charging curve of the MSCs array component, top inset is the circuit diagram of the energy storage mode, bottom inset is the enlarged curve showing the potential rising.

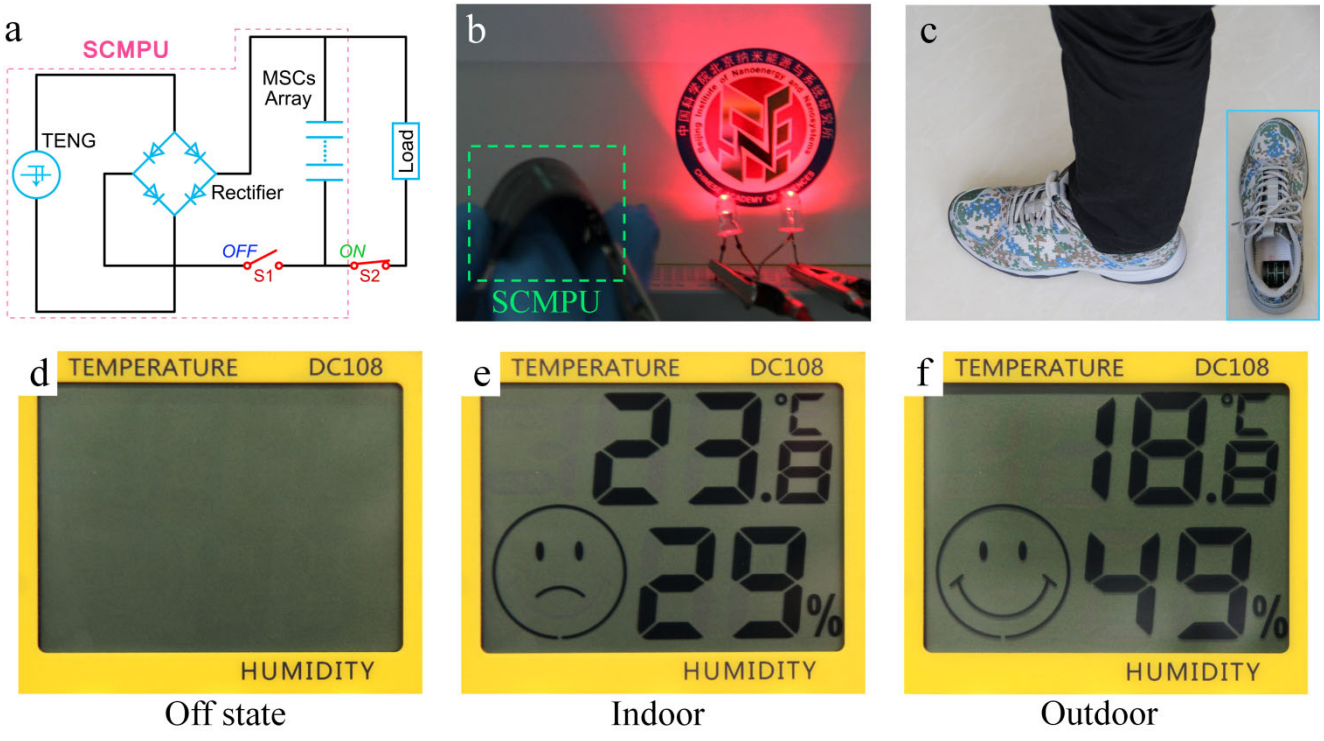

Figure 6 (a) Circuit diagram of the energy supply mode. (b) Photograph showing two LEDs being powered by the SCMPU. (c) Photograph of the SCMPU inserted in the insole. (d-f) Photographs of using the SCMPU to drive a commercial hygrothermograph.

Electronic Supplementary Material

Flexible self-charging power unit by integrating micro-supercapacitor and triboelectric nanogenerator

Jianjun Luo[1,†], Feng Ru Fan[1,2,†], Tao Jiang[1], ZhiweiWang[1], Wei Tang[1], CuipingZhang[1], MengmengLiu[1], GuozhongCao[1,3], Zhong Lin Wang[1,4](✉)

[1]*Beijing Institute of Nanoenergy and Nanosystems, Chinese Academy of Sciences, Beijing 100083,China*
[2]*Collaborative Innovation Center of Chemistry for Energy Materials, College of Chemistry and Chemical Engineering, Xiamen University, Xiamen 361005, China*
[3]*Department of Materials Science and Engineering, University of Washington, Seattle,Washington 98195, USA*
[4]*School of Material Science and Engineering, Georgia Institute of Technology, Atlanta, Georgia 30332,USA*
† These authors contributed equally to this work.

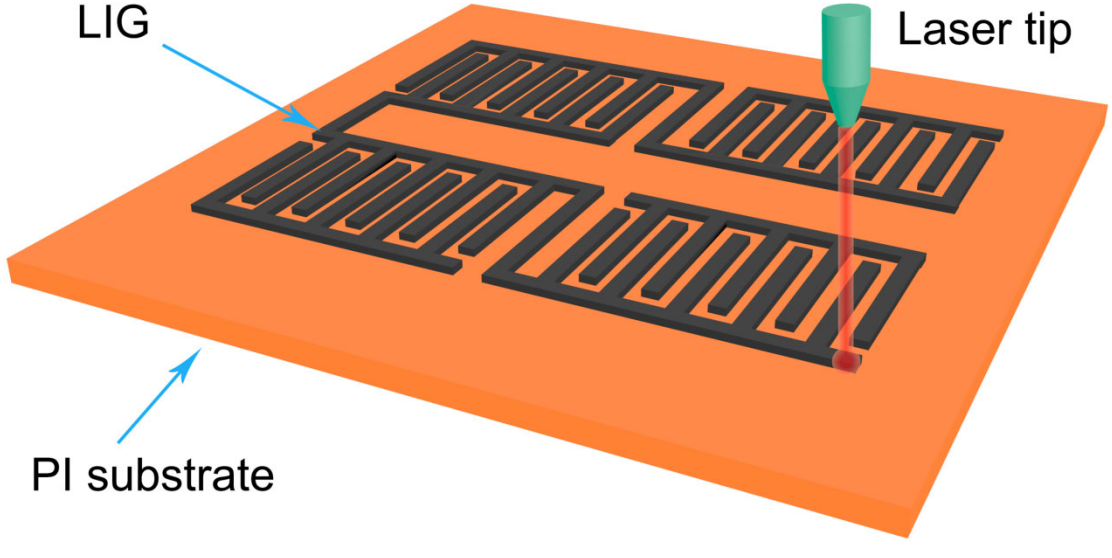

Figure S1 Schematic of the laser engraving process of LIG from the PI substrate.

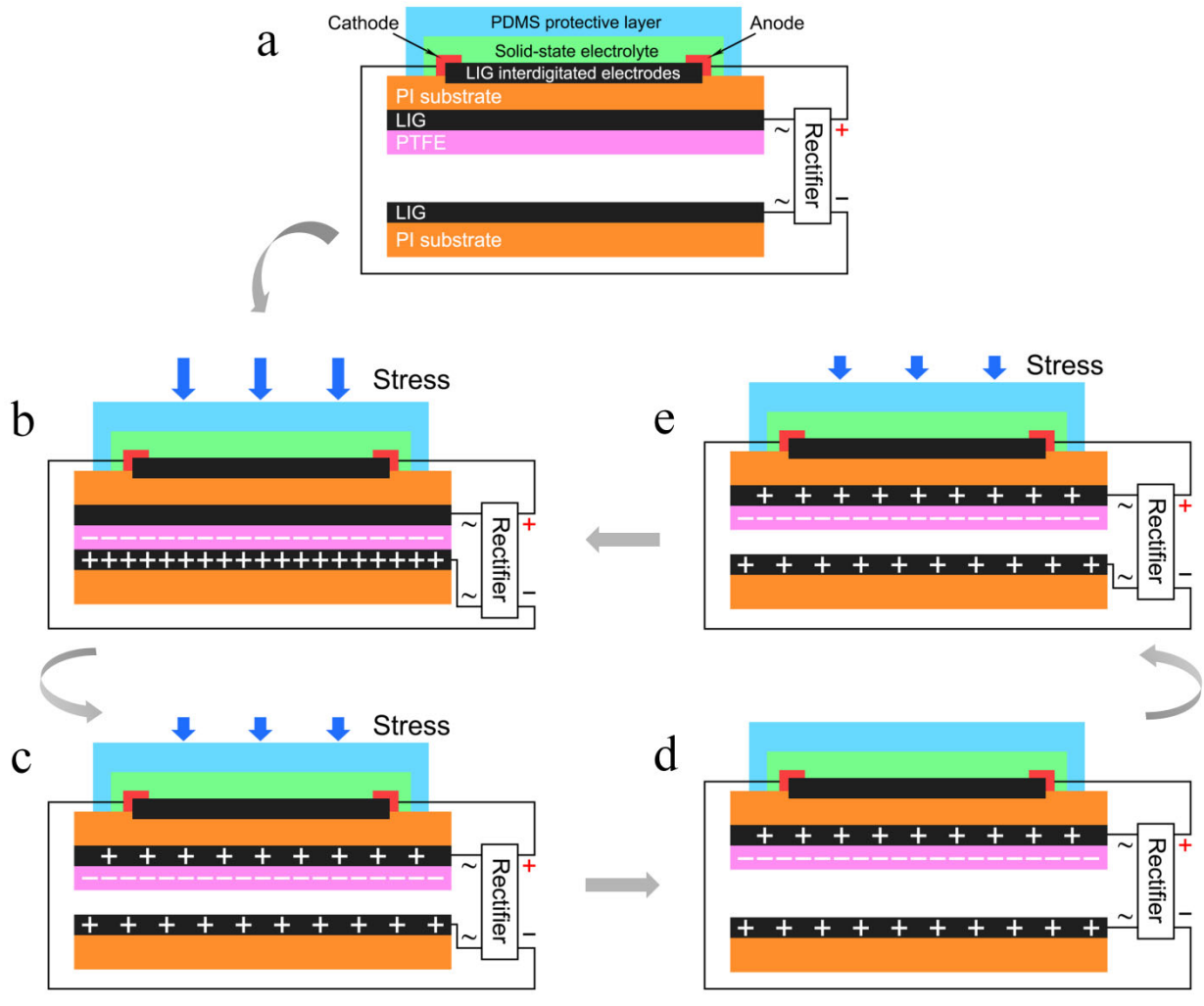

Figure S2 Sketches that illustrate the working principle of the SCMPU. (a) Fabricated SCMPU at the original state before mechanical deformation. For simplicity purposes, the arch-shape is expressed as a flat structure. (b) With an external force, the PTFE and bottom LIG electrode are brought into contact with each other, and opposite triboelectric charges are generated on these surfaces. (c) Mechanical stress is releasing and the SCMPU is reverting back to its original state. The first current peak is generated by the induced potential difference, which charges the MSCs array part. (d) The SCMPU returns to the original state, with induce potential difference fully screened. (e) Once the SCMPU is pressed again, the redundant charges on the bottom LIG electrode flows back. The second current peak is generated to charge the MSCs array part.

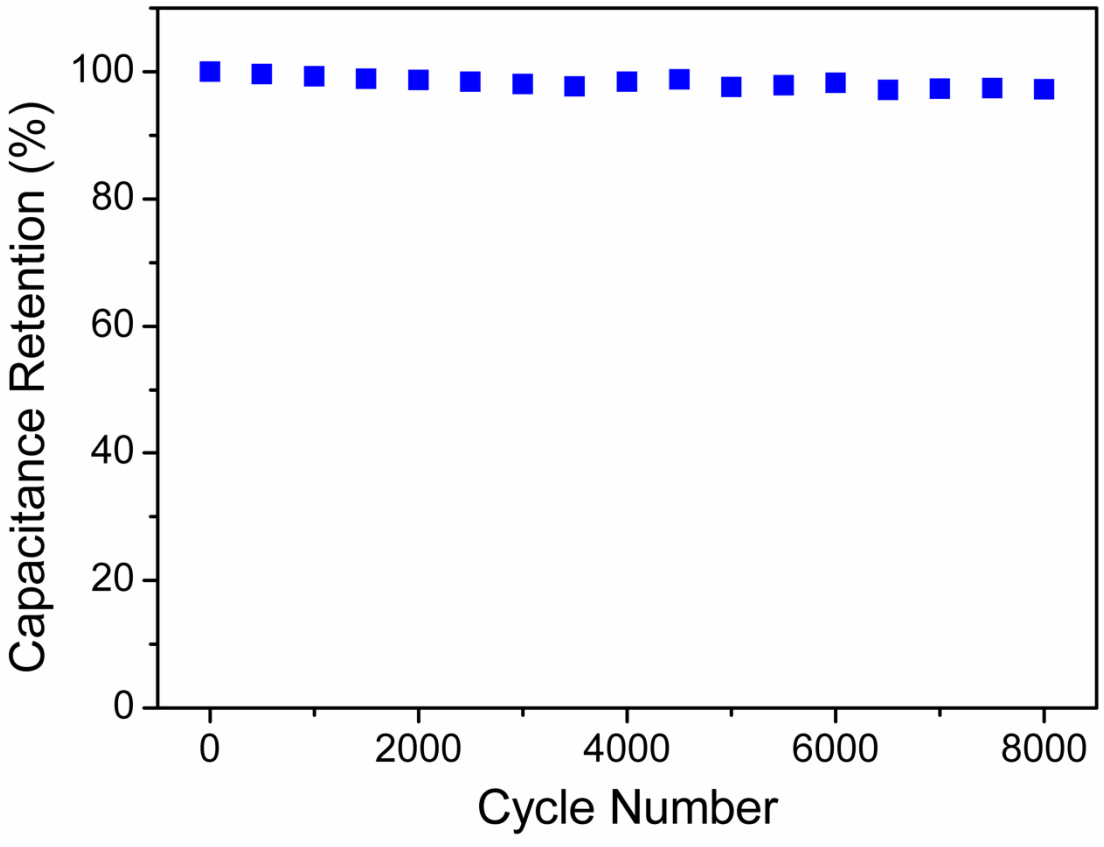

Figure S3 Cyclability testing of MSCs array (four connected in series) with a CC current density of 0.05 mA/cm^2. We can see that the MSCs array shows excellent cycling stability, retaining more than 97% of its initial capacitance after 8000 charge/discharge cycles.

Movie S1 Computer-controlled laser engraving onPI substrates to form LIG.

Address correspondence to zlwang@gatech.edu

Electronic Supplementary Material

Flexible Self-Charging Power Unit by Integrating Micro-supercapacitor and Triboelectric Nanogenerator

Jianjun Luo[1,†],Feng Ru Fan, [1,2,†]Tao Jiang[1],ZhiweiWang[1], Wei Tang[1], CuipingZhang[1], MengmengLiu[1], GuozhongCao[1,3], Zhong Lin Wang[1,4]*

[1]Beijing Institute of Nanoenergy and Nanosystems, Chinese Academy of Sciences, Beijing 100083,China

[2]Collaborative Innovation Center of Chemistry for Energy Materials, College of Chemistry and Chemical Engineering, Xiamen University, Xiamen 361005, China

[3]Department of Materials Science and Engineering, University of Washington, Seattle,Washington 98195, USA

[4]School of Material Science and Engineering, Georgia Institute of Technology, Atlanta, Georgia 30332,USA

[†]These authorscontributed equally to this work.

Address correspondence to zlwang@gatech.edu

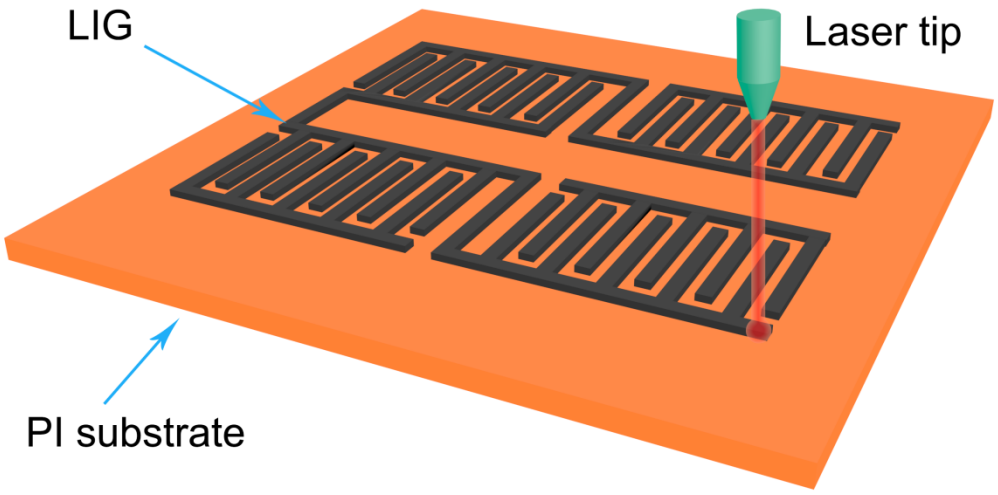

Figure S1 Schematic of the laser engraving process of LIG from the PI substrate.

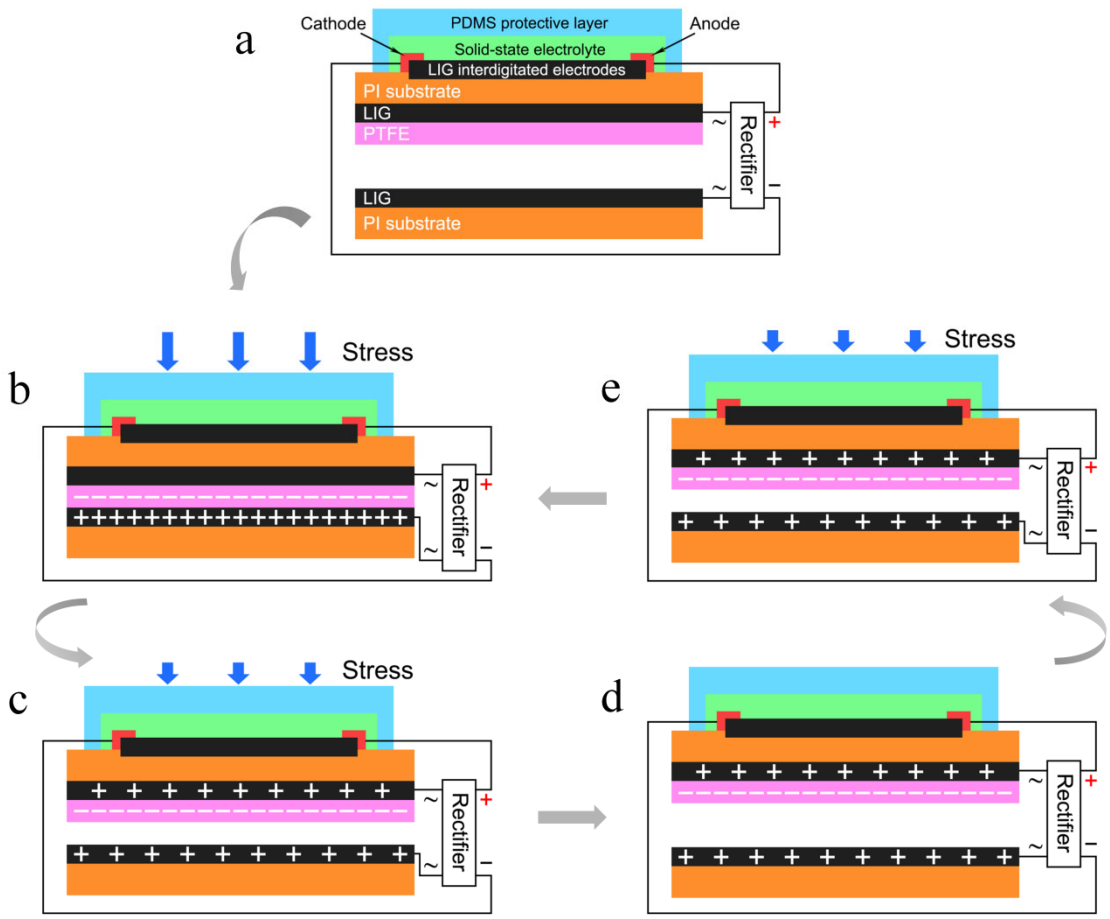

Figure S2 Sketches that illustrate the working principle of the SCMPU. (a) Fabricated SCMPU at the original state before mechanical deformation. For simplicity purposes, the arch-shape is expressed as a flat structure. (b) With an external force, the PTFE and bottom LIG electrode are brought into contact with each other, and opposite triboelectric charges are generated on these surfaces. (c) Mechanical stress is releasing and the SCMPU is reverting back to its original state. The first current peak is generated by the induced potential difference, which charges the MSCs array part. (d) The SCMPU returns to the original state, with induce potential difference fully screened. (e) Once the SCMPU is pressed again, the redundant charges on the bottom LIG electrode flows back. The second current peak is generated to charge the MSCs array part.

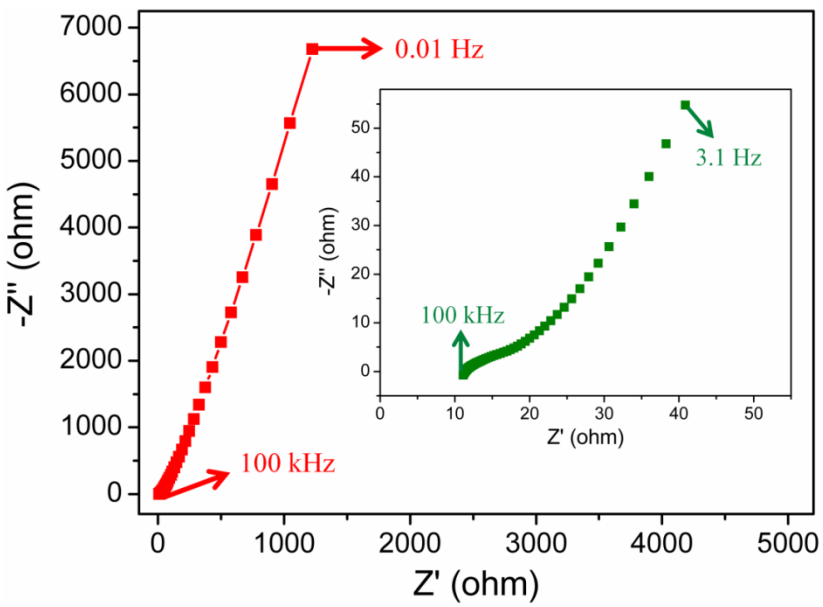

Figure S3 Electrochemical impedance spectroscopy (EIS) characterization of the LIG-MSC. The Nyquist plot shows a small semicircle over the high-frequency range and a near vertical line over the low-frequency range. These results indicatea small charge-transfer resistance and anideal capacitive behavior of the LIG-MSC, respectively.

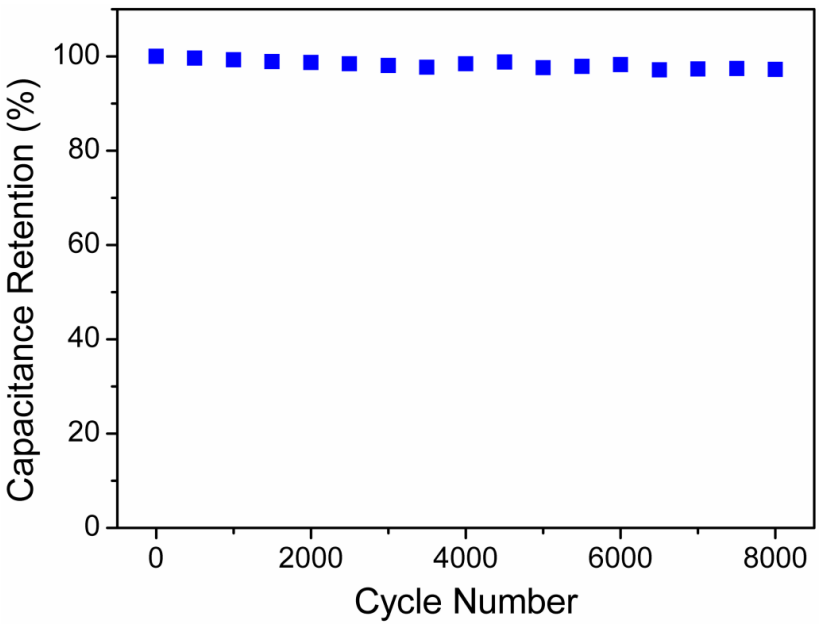

Figure S4 Cyclability testing of MSCs array (four connected in series) with a CC current density of 0.05 mA/cm^2. We can see that the MSCs arrayshows excellent cycling stability, retaining more than 97% of its initial capacitance after 8000 charge/discharge cycles.